

# Surface Initiated Growth of Poly(ethyl 2-cyanoacrylate) Nanofibers on Surface-Modified Glass Substrates

Pratik J. Mankidy,<sup>†</sup> Ramakrishnan Rajagopalan,<sup>‡</sup> Carlo G. Pantano,<sup>‡</sup> and Henry C. Foley<sup>\*,†,‡,§</sup>

Department of Chemical Engineering, Materials Research Institute, and Department of Chemistry, The Pennsylvania State University, University Park, Pennsylvania 16802

Received August 14, 2008. Revised Manuscript Received October 22, 2008

Nanofibers of poly(ethyl 2-cyanoacrylate) were directly grown via a template-less vapor phase polymerization technique directly on surface modified glass substrates. Several commercially available glass slides were investigated for polymer nanofiber deposition. In addition, glass substrates were also modified in the laboratory using silanes with different functional groups. The growth of nanofibers at different relative humidities was studied using scanning electron microscopy (SEM) and atomic force microscopy (AFM). It was found that nanofiber formation is favored when the polymerization occurs at relative humidities greater than 68%. The diameter and the number density of the nanofibers were examined in terms of the wettability of cyanoacrylate monomer on the modified glass substrates.

## 1. Introduction

There is significant fundamental and applied interest in polymer nanofibers as a result of their unique properties and the variety of potential applications they offer. Their utility spans a wide variety of areas, for example, electronics, textiles, and medicine.<sup>1,2</sup> For many of these applications the high surface areas and porosity associated with networks of polymer nanofibers are of significance. The ultimate feasibility of using polymer nanofibers in real applications will depend on our ability to produce them via a facile route, ideally, one which involves few processing steps, provides control over their placement, and which can be extended from laboratory-scale synthesis to larger scale production. Although nanofibers can be prepared using mesoporous silica or porous alumina templates and although this method is truly elegant, the consumption of the rather expensive template with each batch of nanofibers limits the scalability of the process. Therefore, examination of different synthetic routes was warranted. A template-less route to polymer nanofiber synthesis, as demonstrated recently by us<sup>3,4</sup> and others,<sup>5–8</sup>

is a promising route because it can be scaled nicely to and there is no consumption of an expensive template. However, to control the properties of the nanofibers, such as their diameter and aspect ratios, becomes a new challenge in this approach. Rather than using physical confinement, as provided by the template, we must develop chemical methods that provide separate control of the growth kinetics along the fiber axis versus its diameter. This chemical method for polymer nanofibers synthesis is a true “bottom-up” route to synthesis, and it may open up avenues to other new materials. As such it could be an attractive alternative to physical methods such as electrospinning<sup>9,10</sup> and templated fabrication of polymer nanofibers.<sup>11</sup>

To extend this template-less route of making nanofibers further, a protocol for the synthesis of nanofibers on any substrate is desirable. Recently, Doiphode et al.<sup>6</sup> have demonstrated the growth of poly(ethyl 2-cyanoacrylate) [PECA] nanofibers on electrospun microfibers after exposing them to water vapor and then to ethyl 2-cyanoacrylate (ECA) vapor. To explain this phenomenon of nanofiber growth an analogy can be drawn to vapor–liquid–solid growth used for production in whisker technology.<sup>12</sup> Our recent study<sup>4</sup> demonstrated PECA nanofiber growth was achieved readily on solid substrate surfaces by introducing ECA monomer vapor under conditions of high relative humidity (~95%) to substrates surfaces that had been spin coated with appropriate initiators for polymerization. We observed that the morphology of PECA, that is, whether it became a two-dimensional film that was flat or reticulated or if it became high aspect ratio nanofibers, depended on the hard/soft acid base nature of the initiators. Harder anions favored polymer film formation while softer ones favored polymer nanofiber formation.

\* Corresponding author. E-mail: hfoley@ist.psu.edu.

<sup>†</sup> Department of Chemical Engineering.

<sup>‡</sup> Materials Research Institute.

<sup>§</sup> Department of Chemistry.

- (1) Huang, Z. M.; Zhang, Y. Z.; Kotaki, M.; Ramakrishna, S. *Compos. Sci. Technol.* **2003**, *63*, 2223–2253.
- (2) Subbiah, T.; Bhat, G. S.; Tock, R. W.; Parameswaran, S.; Ramkumar, S. S. *J. Appl. Polym. Sci.* **2005**, *96*, 557–569.
- (3) Mankidy, P. J.; Ramakrishnan, R. B.; Foley, H. C. *Chem. Commun.* **2006**, *10*, 1139–1141.
- (4) Mankidy, P.; Rajagopalan, R.; Foley, H. C. *Polymer* **2008**, *49*, 2235–2242.
- (5) Huang, J. X.; Kaner, R. B. *Chem. Commun.* **2006**, 367, 376.
- (6) Doiphode, S. V.; Reneker, D. H.; Chase, G. G. *Polymer* **2006**, *47*, 4328–4332.
- (7) Liu, J.; Lin, Y. H.; Liang, L.; Voigt, J. A.; Huber, D. L.; Tian, Z. R.; Coker, E.; McKenzie, B.; McDermott, M. J. *Chem.-Eur. J.* **2003**, *9*, 605–611.
- (8) Yu, Y. J.; Si, Z. H.; Chen, S. J.; Bian, C. Q.; Chen, W.; Xue, G. *Langmuir* **2006**, *22*, 3899–3905.

(9) Li, D.; Xia, Y. N. *Adv. Mater.* **2004**, *16*, 1151–1170.

(10) Reneker, D. H.; Chun, I. *Nanotechnology* **1996**, *7*, 216–223.

(11) Martin, C. R. *Science* **1994**, *266*, 1961–1966.

(12) Wagner, R. S.; Ellis, W. C. *Appl. Phys. Lett.* **1964**, *4*, 89–91.

**Table 1. Surface Elemental Atomic Compositions of Commercial Glass Slides by XPS**

atomic %	Na	Sn	Cu	O	N	Ca	Mg	K	C	Si	Al
Supramine	4.38			55.39	1.75	1.40	1.16		13.63	21.11	1.19
Schott	0.50			57.25	2.15			1.08	12.73	23.50	1.27
Corning	0.61			59.91	1.12	1.06	0.19		8.24	22.15	5.14
Superfrost	2.89			53.21	1.69	1.55	1.20	0.29	15.22	22.87	1.09
Superclean	2.88	0.44	0.15	53.43		1.52	0.97		16.52	24.08	
Superclean*	1.10			64.85		1.27	0.89		4.55	26.85	0.48

In this work, we have gone further; silanes when used to modify the chemistry of a glass substrate surface become quite effective initiators for growth of PECA nanofibers. This study provides insight into the mechanism of template-less growth of the PECA nanofibers on silane-modified glass substrates. We expect that research of this kind can bring chemical techniques for nanofiber synthesis a step closer to being viable for production.

## 2. Experimental Section

**2.1. Materials.** The following commercially available surface-modified glass slides were used in this work: Supramine (TeleChem Int. Inc.), Schott Nexterion A, Corning GAPS II, and Superfrost Plus (Erie Scientific Company). In addition, unmodified glass slides also available from TeleChem (called Superclean) were used as substrates for silane surface modifications in our laboratory. The silanes used in this study were 3-aminopropyltriethoxy silane (APS), *N*-(2-aminoethyl)-3-aminopropyltrimethoxy silane (AAS) and (3-trimethoxysilylpropyl) diethylenetriamine (DETA), propyltrimethoxy silane (PTS) and methyltrimethoxy silane (MTMS), and (heptadecafluoro-1,1,2,2,-tetrahydrodecyl)trimethoxy silane (HDF), all purchased from Gelest Inc. The chemical structures of the silane molecules are included for reference in the Supporting Information section. Ethyl 2-cyanoacrylate (ECA) purchased from Sirchie Fingerprint Laboratory Inc. was used as the monomer source.

**2.2. Methods.** *Long-Time Polymerization (Fuming).* Polymerization of ECA vapor (also called cyanoacrylate fuming) onto the glass substrates was carried out at room temperature in an enclosed chamber with controlled humidity. The experiment involved two steps: the chamber was first maintained at high relative humidity (~95%) for 10 h followed by the introduction of monomer vapor inside the chamber for polymerization at high humidity for another 10 h. The high relative humidity (RH) was achieved by placing a trough containing an 8 wt % aqueous solution of sulfuric acid in the chamber. A schematic of the enclosed chamber setup is included in the Supporting Information section.

*Different Humidity Fuming.* In these experiments, polymerization of the ECA vapor was carried out under different conditions of relative humidity (RH) in the chamber on the same type of glass substrate (Supramine, TeleChem) for the same amount of time. The first step of the experiment was subjecting the substrate to the particular RH for 10 h which was followed by 2 h of polymerization after the introduction of monomer in the chamber. Polymerization was carried out at five different humidities, 18%, 48%, 68%, 81%, and 94%. These humidities were achieved at room temperature using aqueous solutions of sulfuric acid with concentrations of 62 vol %, 34 vol %, 24 vol %, 17 vol %, and 8 vol %, respectively.

Polymerization experiments were also carried out on the Supramine substrates at 48% RH for different lengths of time (2 h, 6 h, 10 h, and 12 h) using separate substrates and also at 68% RH for different lengths of time (0.5 h, 2 h, 4 h, and 9 h).

*Water Condensation Imaging.* Water condensation on Supramine substrates was imaged using a FEI Quanta 200 Environmental SEM (ESEM) fitted with a temperature controlled stage set at 5 °C. By controlling the pressure in the ESEM sample chamber, the

relative humidity on the surface of the substrate was increased. As the humidity rose above 95% RH, saturation in the vapor phase caused condensation of water droplets on the surface which were then imaged as a function of time.

*Silanation.* Superclean glass cleaned for 1 h in a freshly prepared piranha etching solution (denoted as Superclean\*) was used as the substrate for surface modification by silanes. Silanes were applied from 2% silane solutions in a 95:5, ethanol to water mixture. The silane solution was first allowed to undergo hydrolysis for 1 h and 30 min before introducing the substrate for 30 min. Upon removal, the substrate was rinsed with ethanol and placed in an oven maintained at 110 °C for 2 h to complete the condensation reaction after which the glasses were used immediately for polymerization.

*Characterization.* Field emission scanning electron microscopy (FESEM) was used to observe the morphology and characterize the dimensions of the polymer nanofibers. Atomic force microscopy (AFM) in tapping mode was used to determine the topographical information about the different glass substrates. X-ray photoelectron spectroscopy (XPS) was used to determine the elemental composition of the glass substrate surfaces.

## 3. Results

**3.1. Elemental Analysis by XPS of Commercial Glass Slides.** To assess the elemental composition of the surface of the glass substrates, XPS survey scans were used. Table 1 shows the atom % compositions of the various commercial glass slides used in this study. The compositions are for the as-received glasses except Superclean\* which was "piranha" etched for 1 h.

The compositions of all the glass surfaces except the Schott Nexterion glass are rich in soda lime which is used in their production. One noteworthy observation is that the carbon content for the as-received Superclean slides (16.5 wt %) was significantly reduced to 4.55 wt % by 1 h of soaking in a piranha etch solution. We refer to this as the Superclean\* substrate. The nitrogen content on the amino-silane modified glass substrates ranged from 1.12 wt % on the Corning glass to 2.15 wt % on Schott glass. These mass loadings are consistent with surface coverage of ~1–2 monolayers by the silane.

**3.2. Long-Time Fuming on Commercial Glass Slides.** The commercially available glasses were used as-received in the long exposure time fuming experiments. Additionally, an as-received Superclean glass and a piranha etched Superclean\* substrate were also exposed to the same conditions of polymerization. The development of a white residue visible to the naked eyes was indicative of PECA polymer formation on the substrate surface. The Supramine, Superfrost, and Superclean glasses all developed a white residue during polymerization, while the Corning, Schott, and Superclean\* glasses were transparent to the naked eye under the same conditions and for the same exposure time.

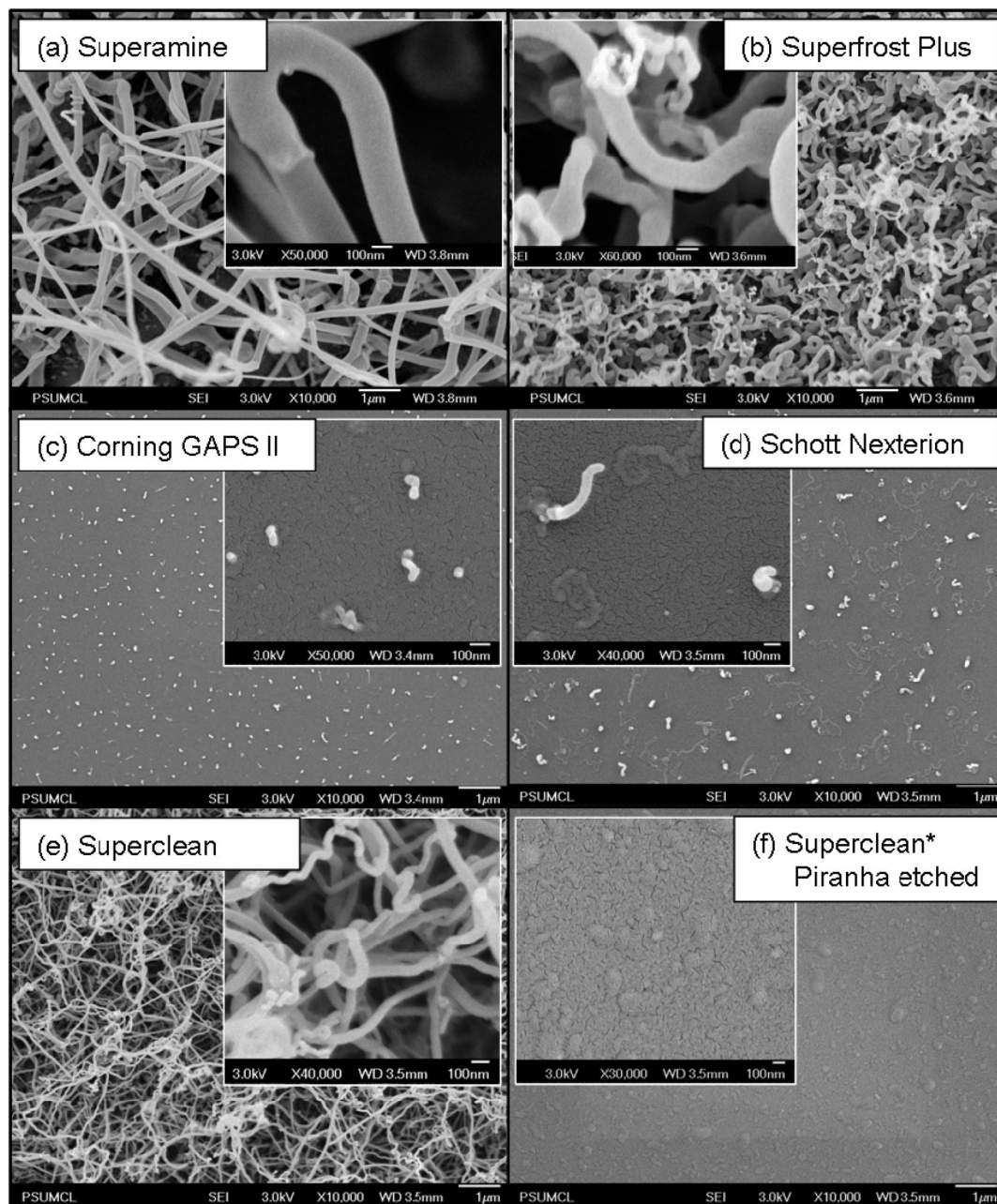


**Figure 1.** SEM Image results of long-time fuming on (a) Superamine, (b) Superfrost Plus, (c) Corning GAPS II, (d) Nexterion A Schott, (e) Superclean, and (f) Superclean\*. Scale bars = 1  $\mu\text{m}$ . Inset Scale bars = 100 nm.

In Figure 1, we present the SEM images of the surfaces of the six glass slides after polymerization. The three slides that had a visible white polymer deposit, when viewed under the SEM, show dense masses of polymer nanofibers. The fibers on the Superamine substrate had diameters ranging from 100 nm to 300 nm. The fibers grew into an entangled branched network making it difficult to estimate their lengths, but they appear to be greater than several tens of micrometers long. Nanofibers deposited on the Superfrost Plus glass appear to be more coiled than those on the Superamine glass. The diameters here ranged from 50 nm to 300 nm. The fibers on the Superclean glass appeared similar to the fibers on the Superamine glass and have diameters ranging from 50 nm to 200 nm. The Corning and Schott glasses, when viewed under the SEM, showed short polymer nanofibers sparsely dispersed on

the substrate surface. Under high magnification the diameters of the fibers on the Corning glass appeared to be monodisperse with a narrow distribution of diameters centered at  $\sim 50$  nm. The fibers on Schott glass also appeared to have monodisperse diameters but centered about a mean of  $\sim 100$  nm. Comparing the number density (number of fibers per unit area), the Corning glass substrate has a slightly greater density of polymer fibers deposited than the Schott glass substrate. The image of the surface of the Superclean\* glass does not show the formation of any polymer nanofibers; however, there was some localized deposition of thin polymer film at different places across the substrate surface. The extent of film deposition on the Superclean\* glass was fairly insignificant when compared to the extents of deposition on Superamine, Superfrost, and Superclean glasses.



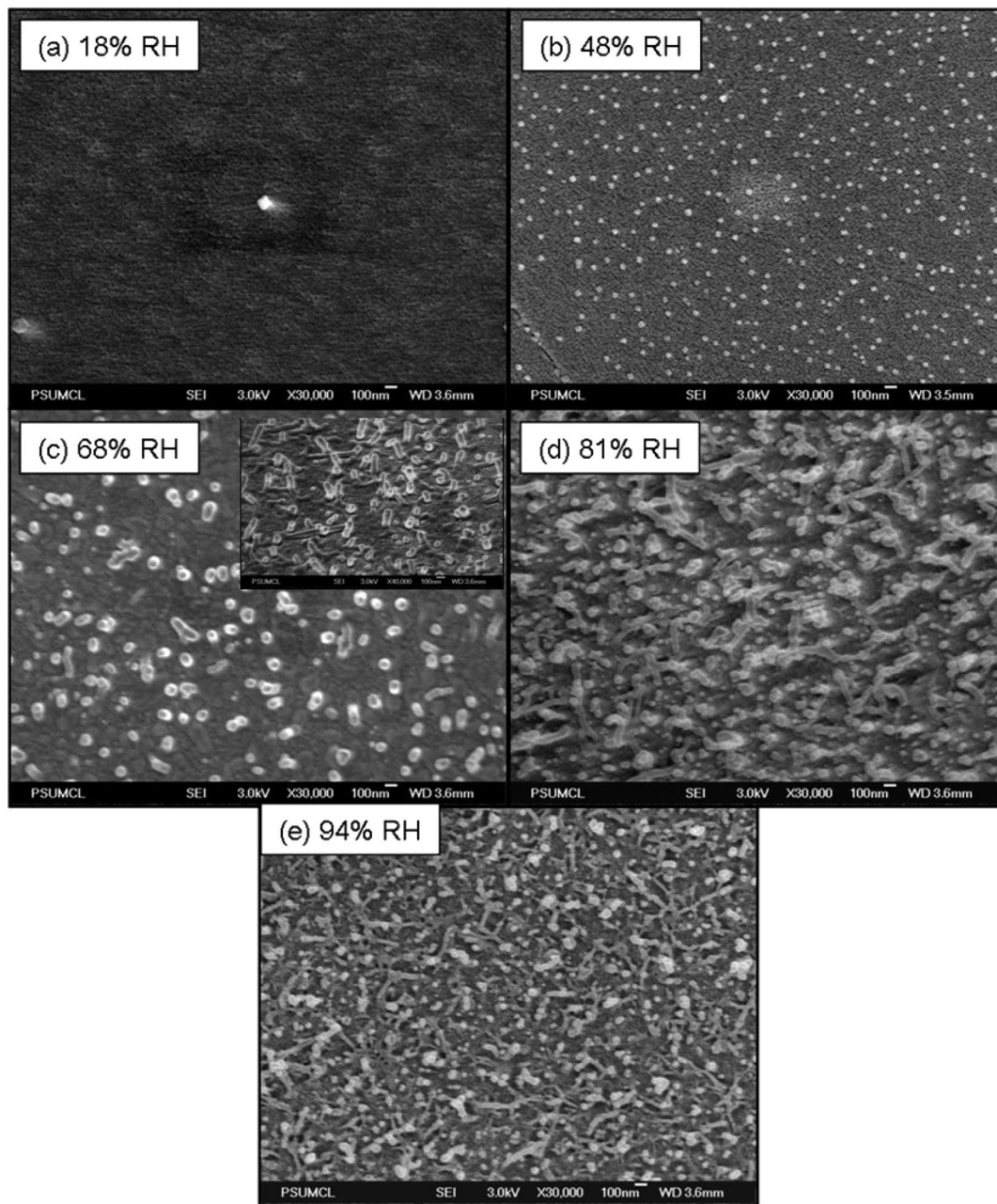


**Figure 2.** PECA polymer growth on Superamine glass substrates at 2 h of polymerization under different relative humidities.

### 3.3. Variable Humidity Fuming on Superamine Glass.

To capture the onset of polymer deposition, Superamine glass substrates were subjected to 2 h of fuming with ECA vapor and at different humidities. The substrates that were subjected to fuming at relative humidities of 18%, 48%, and 68% did not develop any white polymer residue as seen by the naked eye, while those fumed at 81% and 94% RH samples did develop a faint white deposit, which was observable. In Figure 2, we present the SEM images of the surface of the Superamine substrates after 2 h of polymerization subjected to different relative humidities. The glass under 18% RH shows very few nubbins, or buds, of polymer deposited on the surface. At 48% RH, the number of the polymer buds deposited on the surface increased; the size of each bud was  $\sim 60$  nm, and they were fairly uniform in size across the entire glass surface. When the RH was increased to 68%, we observed short

stubs of polymer nanofibers for the first time. SEM images of these short polymer stubs taken at a tilt angle of  $45^\circ$  showed that the diameters of the stubs were between 50 and 100 nm and that the lengths of the polymer stubs extended up to 200–250 nm. When the RH was increased further to 81%, we clearly saw the formation of longer nanofibers in the same 2 h time period for polymerization. The fiber diameters were once again in the range from 50 to 100 nm, but now we noted some branching of the fibers also becomes evident. Comparing these fibers with those synthesized at 94% RH (Figure 2e), we observed that the fibers grown at 94% RH were even longer than those grown at 81% RH for the same time period and with higher humidity there was even more branching, but interestingly, the range of nanofiber diameters remained nearly the same between 50 and 100 nm diameters.

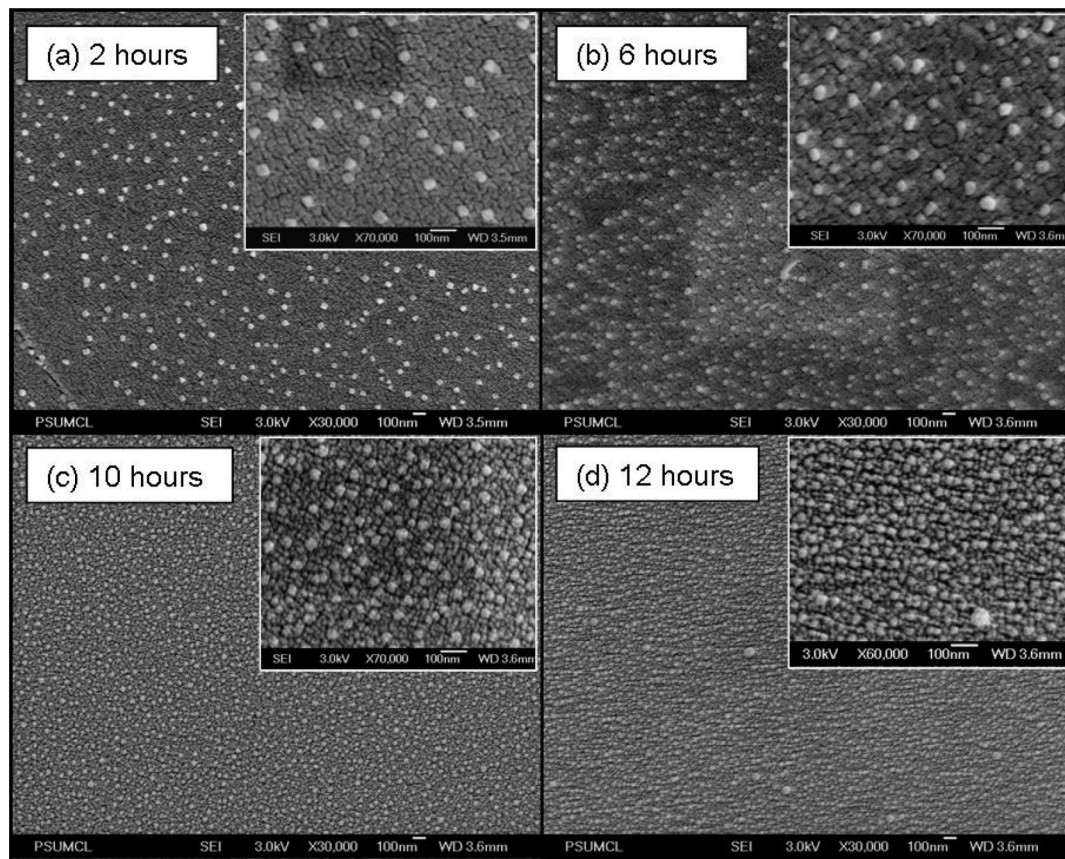


**Figure 3.** Polymer bud deposition on Superamine glass substrates under 48% RH at various time periods of fuming. Scale bar = 100 nm.

To investigate the development of the polymer nanofibers further, we repeated the polymerizations at 48% RH and 68% RH on Superamine substrate, but now as a function of time. In Figure 3a–d we see the SEM images of the polymer that was deposited on the Superamine substrates during polymerization under 48% RH for 2, 6, 10, and 12 h, respectively. There is a noticeable difference between the image taken at 2 h and that taken after 6 h of polymerization, in that there were noticeably more polymer buds at the longer time. Although their number density increased, the size of the polymer buds was constant at  $\leq 60$  nm. The same trend was observed in going from the 6 h sample to the 10 h sample image as more small buds appear on the surface. After 12 h of exposure to the ECA monomer vapor, the density of the polymer stubs increased to such an extent that they appear to almost completely cover the glass substrate surface.

The SEM images of the surface of the Superamine glass after 0.5, 2, 4, and 9 h of polymerization under 68% RH are presented in Figure 4a–d. After 0.5 h, short polymer nanofibers with diameters ranging from 30 to 50 nm and with lengths of  $\sim 200$  nm were clearly evident. As the exposure time to ECA vapor was increased to 2 h, the resultant fibers appeared to be unbranched and to have grown nearly vertically (perpendicular to the surface) and with the diameter ranging from 50 to 100 nm. At 4 h, the fibers grew longer and now appeared to be branched. After 9 h of polymerization, there were many more of the branched nanofiber structures and the diameters of the fibers varied from 50 nm to 100 nm.

**3.4. AFM Imaging on Commercial Glass Slides.** To capture the onset of polymer deposition on the glass substrates, AFM imaging was also performed on the Superamine, Schott Nexterion, and Corning GAPS II glasses before and after polymerization under 48% RH. Figure 5 shows AFM height images of the (a) as-received Superamine glass surface and (b) same surface after 2 h of polymerization, under 48% RH. The as-received Superamine glass is a smooth surface with no major topographical features. After 2 h of polymerization a large number of 60 nm polymer buds were deposited on the surface. The 3D view of the height image illustrates that the polymer buds on average measured about 100 nm in height. The results are in agreement with the interpretation of the SEM images in Figure 3a.

The AFM height images of the (a) as-received Schott Nexterion glass surface and (b) same surface after 10 h of polymerization under 48% RH are shown Figure 6. As in the case of the Superamine glass surface, the as-received Schott glass was a smooth surface with absolutely no apparent features (Figure 6a). After 10 h of polymerization (Figure 6b), there was evidence for polymer deposition on this substrate as shown by a few white dots on the surface.

In the case of Corning GAPS II glass slides (Figure 7), the as-received substrate surface showed a large population of evenly dispersed “silane islands”.<sup>13</sup> The diameter of these islands was 50 nm, or smaller, and their height was roughly 5 nm. After 5 h of polymerization under 48% RH, the surface

(13) Eromosele, I. C.; Pepper, D. C.; Ryan, B. *Makromol. Chem.* **1989**, *190*, 1613–1622.



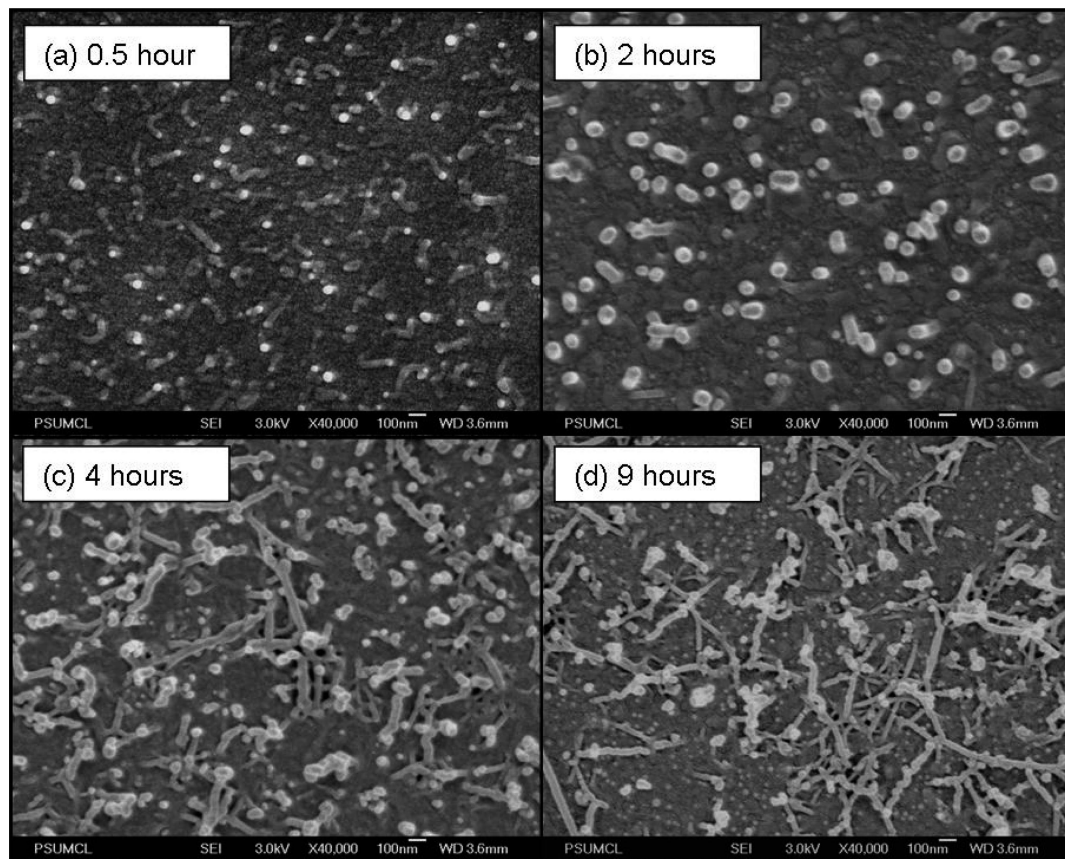


**Figure 4.** Polymer nanofiber growth on Superamine glass substrates under 68% RH at various time periods of fuming. Scale bar = 100 nm.

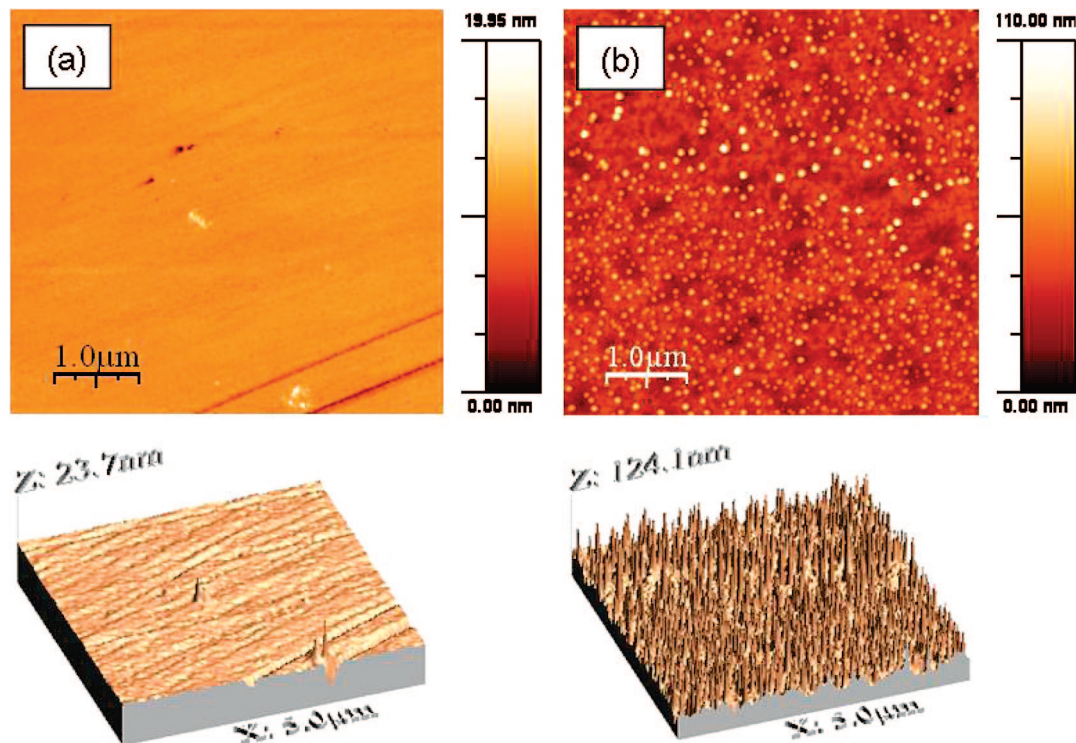


**Figure 5.** AFM height images of (a) as-received Superamine glass and (b) Superamine glass after 2 h of polymerization under 48% RH.

showed only very sparse polymer deposition as indicated by the AFM image.

**3.5. Water Condensation Imaging on Superamine Glass.** As water is a known initiator for ECA polymerization,<sup>14</sup> we investigated the physical process of formation of

water droplets during condensation on a Superamine substrate to see if it correlates with the diameter of the polymer nanofibers. Parts a–d of Figure 8 are ESEM images of the surface of the Superamine substrate taken as water condensed on it at a relative humidity > 95%.

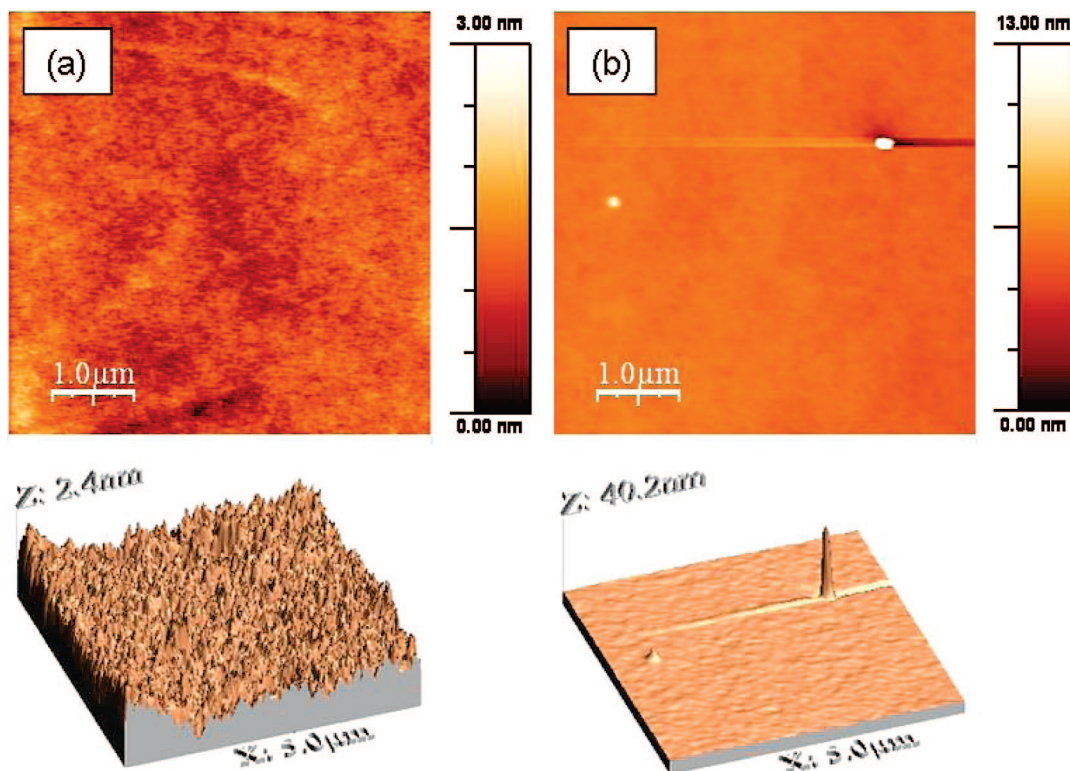


Figure 6. AFM height images of (a) as-received Schott glass and (b) Schott glass after 10 h of polymerization under 48% RH.

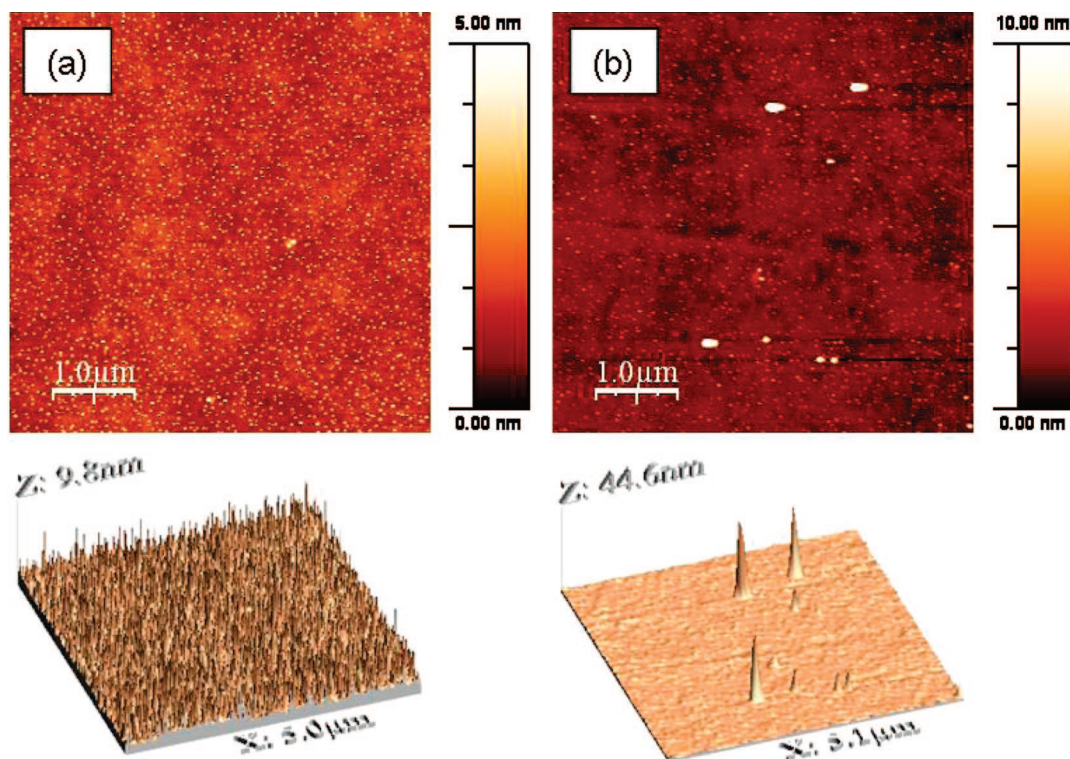


Figure 7. AFM height images of (a) as-received Corning glass and (b) Corning glass after 5 h of polymerization under 48% RH.

The images show a progressive nucleation and growth of water droplets condensing on the surface. In the right-hand portion of the image taken after 30 s of exposure to water vapor, a collection of water droplets having a diameter of  $\sim 500$  nm had appeared, while at the same time larger droplets (several micrometers) were already present. After observing this collection of droplets for a longer period of

exposure to water vapor (at times of 40, 75, and 110 s respectively), the drops were found to grow at about the same rate until they eventually pooled together to form larger water puddles or reservoirs on the surface. There was no clear correlation between sizes of the water droplets which condensed on the substrate surface and the diameter of the polymer nanofibers grown on the same surface.



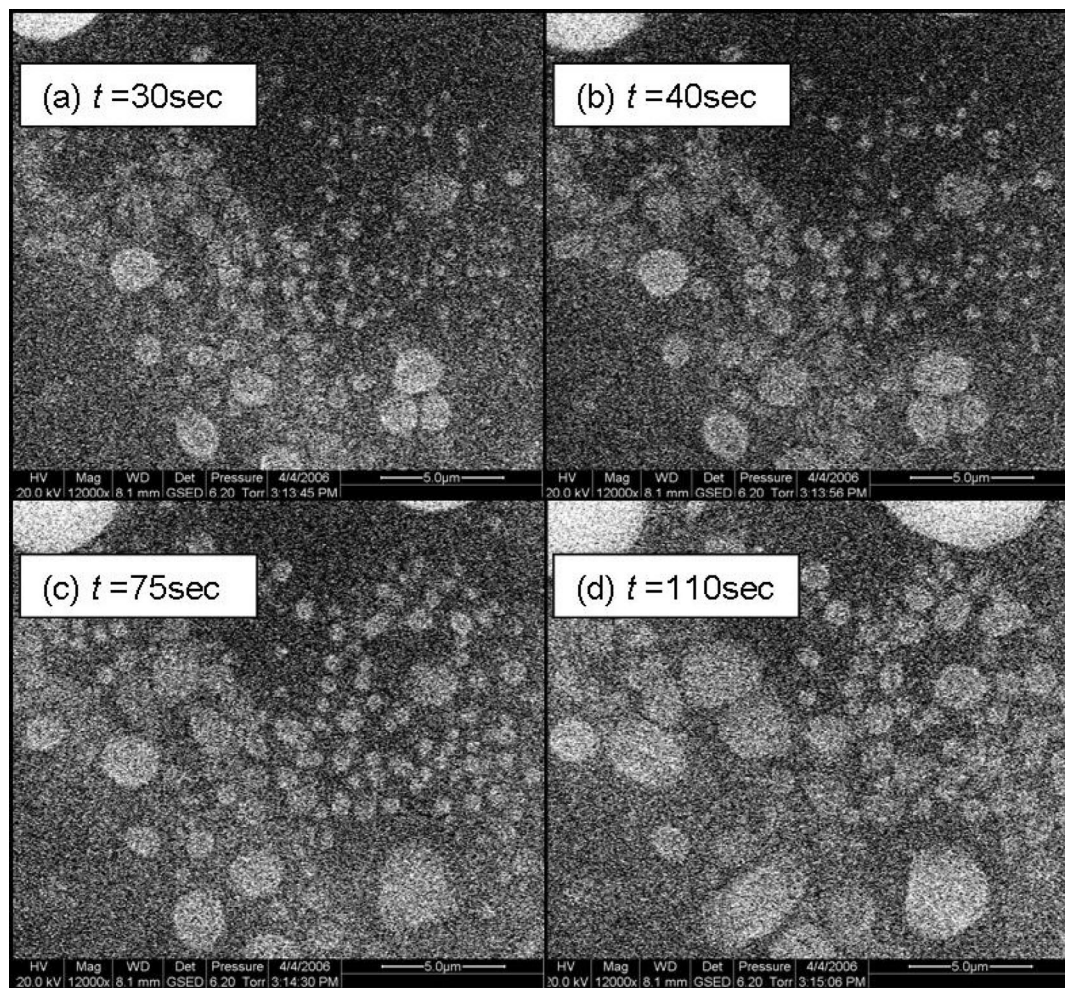


Figure 8. ESEM images of water condensation on Superamine glass substrate at >95% RH. Scale bar = 5  $\mu$ m.

Table 2. Surface Elemental Atomic Compositions of Silane Modified Glass Substrates

atomic %	Na	O	Sn	F	N	Ca	Mg	K	C	Cl	Si	Al
APS on Superclean*	1.17	49.42			2.31	0.86	0.76		19.24	0.32	25.39	0.54
AAS on Superclean*	1.34	51.00			2.68	0.86	0.56		16.72	0.30	25.89	0.66
DETA on Superclean*	1.19	47.25			3.84	0.77	0.72		21.66	0.32	23.83	0.43
MTMS on Superclean*	2.00	55.26	0.3			1.09	0.70	0.18	14.65		25.04	0.81
PTS on Superclean*	1.55	55.88	0.28			1.15	0.61	0.23	13.73		26.40	
HDF on Superclean*	1.49	54.44	0.80	2.00	1.01	0.92	1.15	0.39	12.63		24.70	0.46

**3.6. Long-Time Fuming on (Laboratory-Prepared) Silane Modified Glass.** In order to further understand the role of surface modification of glass, we coated several of the Superclean\* slides with different silanes. Table 2 presents the surface elemental compositions in atom % of the laboratory-prepared silane-modified glass surfaces. The nitrogen content of the three aminosilanes as expected increased in the order APS < AAS < DETA for the mono-, di-, and triaminosilanes, respectively. The nitrogen content for the APS coated Superclean\* was 2.3%, which was slightly greater than the value expected for an APS monolayer ( $\sim 1.5\%$ ) as observed by Metwalli et al.<sup>15</sup> Also the fact that the carbon content for APS treated glass was greater than the carbon content of the AAS treated substrate and the carbon contents of the MTMS treated glass was greater than PTS indicated the formation of multilayers of silane on these substrates.

Next a set of Superclean\* substrates was treated with, APS, AAS, DETA, PTS, MTMS, and HDF and then these surface-modified substrates were fumed with ECA at 95% RH for longer time periods. The results from these polymerization experiments are presented by SEM images representative of the entire glass surface in Figure 9. APS, AAS, and DETA on Superclean\* each resulted in similar polymer nanofiber formation. The fibers had diameters of  $\sim 50$  nm and appeared to be in the initial stages of formation of a network made up of a dense mass of polymer nanofibers. The glass substrates coated with PTS, MTMS, and HDF also displayed nanofibrous polymer; however, the number density of the fibers was less than that on the substrates treated with the aminosilanes. Even for the substrates modified with the nonaminosilanes, the number density of nanofibers decreased in the order PTS > MTMS > HDF. However, the diameter of the fibers still remained constant at roughly 50 nm.



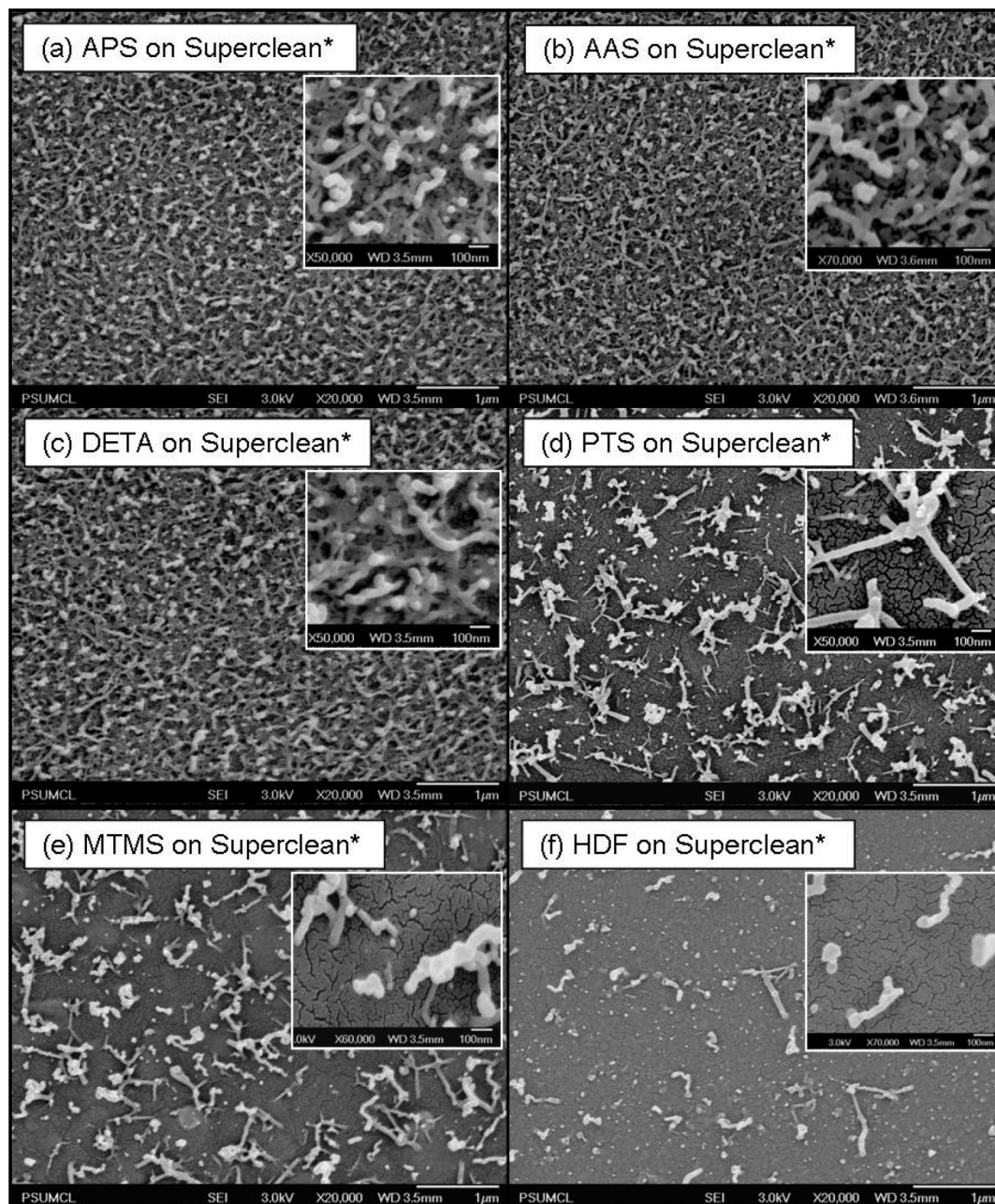


**Figure 9.** SEM Image results of long-time fuming on (a) APS, (b) AAS, (c) DETA, (d) PTS, (e) MTMS, and (f) HDF all on Superclean\*. Scale bars = 1  $\mu\text{m}$ . Inset Scale bars = 100 nm.

#### 4. Discussion

**4.1. Polymerization on Commercial Glass Slides.** The large number density of fibers on the Supramine and Superfrost substrates as compared to the Schott and Corning glass substrates, (Figure 1a–d) for the same time of fuming under the same conditions suggests that there were fewer nucleation sites for initiation of polymer nanofiber formation on the Schott and Corning glass substrates. These substrates have a proprietary composition, but it is known that they are surface-modified with amines since they are used for DNA microarray analysis<sup>16,17</sup> and for increased adhesion in

tissue growth.<sup>18</sup> This presence of the amines at the surface of these commercial substrates is supported by the XPS analysis of them, which indicated the presence of nitrogen in requisite quantities to provide complete surface coverage (Table 1). However, the atomic % of nitrogen does not correspond one-to-one with the number density of PECA fibers observed after fuming. The Supramine and Superfrost substrates having nitrogen contents of 1.75 and 1.69%, respectively, result in the dense growth of nanofibers. By contrast, the Corning and Schott glass substrates with 1.12

(14) Turroni, S. G.; Olmos, D.; Gonzalez-Benito, J. *Polym. Test* **2005**, *24*, 301–308.

(15) Metwalli, E.; Haines, D.; Becker, O.; Conzone, S.; Pantano, C. G. *J. Colloid Interface Sci.* **2006**, *298*, 825–831.

(16) Stears, R. L.; Martinsky, T.; Schena, M. *Nature Medicine* **2003**, *9*, 140–145.

(17) Tech. Information: [http://www.us.schott.com/nexterion/english/products/coated\\_substrates/slide\\_a/technical\\_information.html](http://www.us.schott.com/nexterion/english/products/coated_substrates/slide_a/technical_information.html), Schott North America, 2007 (accessed 2007).

(18) Tech. Information: [http://www.eriesci.com/microscope/micro\\_slides.aspx?id=6](http://www.eriesci.com/microscope/micro_slides.aspx?id=6), Erie Scientific Company (accessed 2007).

and 2.15% nitrogen content, respectively, yielded relatively few nanofibers. In the case of the as-received Superclean glass substrate, although there was no detectable nitrogen on the surface, a dense mass of polymer nanofibers was observed to grow upon it. This indicates that the initiation of formation of the polymer nanofibers on these substrates is independent of their surface nitrogen content. It is significant to take note of the fact that the carbon content of the as-received Superclean slides (16.52%) was actually quite high compared to that which would be expected for a truly clean glass surface, that is, 0%. Hydrocarbon contamination from typical laboratory environments<sup>19</sup> is the most likely source of this carbonaceous deposit as these slides were used after exposure to the air. Once these slides are piranha etched, a technique used to clean surfaces of carbon, the carbon content does drop, but only down to 4.55% (on the Superclean\*) which indicates that although there was significant removal of the majority of the carbonaceous contaminants, a significant amount of carbon remained on the surface. After cleaning the surface of the Superclean substrate in this way, it does *not* initiate polymerization of PECA nanofibers. This indicated that the carbonaceous surface contamination actually was a source of initiators for nanofiber formation.

The requirement of high relative humidity for PECA nanofiber formation was recently reported by us,<sup>3</sup> and it has also been reconfirmed in this study with the short time fuming experiments on Supramine glass under different RHs. Water plays a cocatalytic role in the polymerization of ECA; for the same polymerization time period of 2 h, the extent of polymer deposited on the substrate surface went from few polymer buds noticed at 18% RH, to a larger number of buds at 48% RH, to short fiber stubs at 68%, to longer fibers at both 81% RH and 94% RH. This indicates that initiation of polymer nanofibers occurred at ~68%RH or above, but it progressed faster in the axial direction at the higher relative humidities. Previous studies<sup>6</sup> have suggested that condensation of tiny water droplets on the substrates surface at high relative humidity serves to create islands of initiation that in essence “template” the formation of a bud of PECA with a diameter close to that of the nanofibers which subsequently form. Adsorption of additional ECA vapor then takes place preferentially at the active sites of this bud, and these sites are oriented in such a way that growth occurs largely perpendicular to the substrate surface. This scheme of water condensing on the substrate, to provide a locale for ECA initiation, would not seem to be the case based upon two of our experimental observations. First, during imaging of pure water vapor condensing on the Supramine substrate in the ESEM (Figure 8), the nucleation of water droplets on the surface was observed to be progressive. Such nucleation behavior results in droplets of different sizes being present on the surface at any time, ranging from few hundred nanometers to greater than 2  $\mu\text{m}$ . If in fact ECA initiation were to occur on such a surface with each droplet or pool of water serving as an initiation island, it would result in fibers with diameters of that same size or larger sprouting from the surface. This however is

not observed. In Figures 2c–e and 3, the PECA nanofibers all appear to have relatively consistent diameters between 100 and 200 nm. Second, for the case of fuming on the Superclean\* slide that was etched with piranha solution for 1 h to remove hydrocarbon contamination,<sup>20</sup> there occurred only very limited polymer film deposition even with ECA fuming done for very long times. The piranha etching step, by cleaning the glass surface, made the substrate quite hydrophilic<sup>13</sup> and, hence, thermodynamically quite favorable for water adsorption and condensation. Consequently, there should have been large amounts of PECA polymer film deposition on this substrate if water droplet formation were critical in the process. However, extensive polymer film deposition did *not* occur on this substrate; instead only a rather thin polymer film formed locally in only a few places on the surface and in quantities that were almost negligible enough as to approach zero when compared to the dense masses of polymer nanofibers deposited on other glass substrates. These specifics suggest a more complex mechanism for polymer nanofiber initiation on these substrates.

A review of the SEM images for fuming on the Supramine substrates under 48% RH and 68% RH for different times (Figures 3 and 4) suggests the following hypothesis for polymer nanofiber initiation. We hypothesize that for surfaces which will grow polymer and nanofibers, it is the adsorption of ECA monomer vapor on the surface that is the first step, and then in the subsequent step water vapor adsorption initiates the deposition of polymer occurs. If this is the case, then at 48% RH, the concentration of water vapor on the surface populated with ECA is low, and hence, the ECA is only slowly converted into polymer buds. As time progresses, more ECA polymer buds are deposited in the same way across the surface. However, the polymer buds do not propagate rapid formation of nanofibers at this low humidity level. At this humidity, the rate of termination becomes comparable to the slow initiation and propagation rate of ECA polymerization. Hence the size of the individual polymer buds does not change appreciably, but their number density does increase with time. By increasing to 68% RH or higher, the initiation rate increases since that much more initiator (water vapor) is present. Under these conditions, the initiation and propagation rates are much faster than rate of termination. The living chains of the deposited polymer at the surface of the buds are thus able to sustain nanofiber growth through an insertion polymerization mechanism. This hypothesis is also supported by all the observations we have made in the set of 2 h fuming experiments including those at 18% RH, 81% RH, and 94% RH (Figure 2a,d,e). Recall that at the lowest humidity (18%) very few polymer buds are formed due to insufficient initiator being present, while at the higher humidities (81 and 94%) and for the same fuming time, propagation has ensued to such an extent that long polymer nanofibers are formed.

In accordance with this hypothesis for the same conditions of relative humidity and time of fuming, the number density of polymer initiation sites on a surface should depend on

(19) Smith, G. C. *J Electron Spectrosc.* **2005**, *148*, 21–28.

(20) Shirai, K.; Yoshida, Y.; Nakayama, Y.; Fujitani, M.; Shintani, H.; Wakasa, K.; Okazaki, M.; Snauwaert, J.; Van Meerbeek, B. *J. Biomed. Mater. Res.* **2000**, *53*, 204–210.



the wettability of the ECA monomer on that surface. This conjecture implies that a surface with low wettability for ECA would yield a lower number density of polymer initiation sites. This is verified by the results from the Superamine, Schott, and Corning glass substrates. The AFM images of the same moderate humidity (48% RH) fuming experiments on Superamine, Schott, and Corning (Figures 5–7) revealed that PECA deposition occurred on the Superamine substrate the quickest (within 2 h) followed by deposition on the Corning substrate (within 5 h) and last on the Schott glass substrate (within 10 h). This observation that the ECA preferentially wets the substrates in the order Superamine > Corning > Schott, not only explains the differences in number density of polymer fiber growth, evident on these substrates at long times (Figure 1), but also explains the differences in the extent of polymer deposition. In other words a substrate with good ECA wettability has a greater density of polymer nanofibers than that substrate which does not adsorb ECA well.

This hydrophobicity of the as-received Superclean glass (Figure 1e) is caused by the hydrocarbon contamination present on its surface due to exposure to the ambient laboratory environment. Since such a hydrophobic surface would prefer to adsorb a nonpolar (hydrophobic) molecule, in this case, it adsorbs ECA monomer preferentially to water vapor.<sup>21</sup> Once adsorbed on the surface, the ECA provides the sites for initiation of the PECA nanofibers, as is evident in the SEM images. When cleaned with a piranha etching solution (Superclean\*), the substrate is made hydrophilic since it is now devoid of the hydrophobic contaminant; hence, ECA adsorption is unfavorable and is suppressed. Thus on this very clean, water-adsorbing surface, no fiber formation takes place (Figure 1f). In fact, not only does nanofiber formation *not* occur, but consistent with this hypothesis very little polymerization in any mode occurs. On the Superclean\* substrate rather little polymerization takes place because there is so little ECA present either on the substrate surface or on the surface of a condensed water droplet or layer. In essence, we are arguing that the thermodynamics of ECA adsorption is critical to the kinetics of polymerization. Presumably, there is also a delicate balancing between water adsorption and the ECA adsorption, which both lead to a favorable equilibrium site size due to the thermodynamics of wetting and to favorable polymerization kinetics, which taken together can lead to a fiber growth away from the surface and with diameters that are all similar in size and controlled by the thermodynamics of formation of the ECA-H<sub>2</sub>O nests at the surface. We also know that by varying the partial pressure of water vapor above a critical threshold, we can produce simple two-dimensional films, complex 2·*n* dimensional nanotextured films of the intriguing three-dimensional nanofibers.

The occurrence of Y-shaped branching on some of the nanofibers, like the ones seen in the SEM image of the polymer grown on the Superfrost substrates, must arise either from secondary initiation occurring on a growing nanofiber after a chain transfer step. Also that some of the fibers that

have larger diameters (>100 nm) than the mean value may be the result of continued polymerization wherein now the fibers not only increase axially but also begin to grow radially, with longer polymerization time. But more likely, and in keeping with our hypothesis, there is a distribution of ECA-H<sub>2</sub>O nest diameters around the mean diameter, which is the most favorable value. Although we favor the latter explanation for larger nanofiber diameters, our results do not exclude either possibility.

**4.2. Polymerization on Laboratory-Prepared Silane Modified Glass Surfaces.** Gauging from the elemental composition of the laboratory-prepared silane coated slides, the treatment with various silanes exceeded monolayer coverage on the surface and thereby definitively altered their surface properties. This fact is evident in the results obtained from the long-time fuming experiments on these modified substrates (Figure 10). For the same conditions and time of fuming, the number density of fibers on these substrates decreased in the order of aminosilanes > PTS > MTMS > HDF. This variation can again be explained by the ECA wettability criteria stated above. A review of the expected critical surface tension values ( $\gamma_c$ ) for soda lime glass treated with these particular silanes, obtained from the literature,<sup>22,23</sup> reveals that these values decrease in the same order. The values for  $\gamma_c$  (in mN/m) for APS, AAS, PTS, MTMS, and HDF are reported to be 35, 33.5, 28.5, 22.5, and 14.9 mN/m, respectively. To obtain good wettability of a liquid on a surface, the surface tension of the liquid must be below the critical surface tension of the surface. Hence comparing these values with the surface tension value for ECA monomer,<sup>21</sup> which is 34.32 mN/m, it is clear that in going from the aminosilanes to alkylsilanes and finally to fluorosilane, the ECA wettability and therefore adsorption on the surface decreases. This drop in the magnitude of  $\gamma_c$  would be expected to cause fewer polymer initiation sites on the low  $\gamma_c$  surfaces, which is the observed case. These support our hypothesis for nanofiber formation as arising from the critical wetting of the surface with ECA first, to which water adds above a critical humidity (vapor pressure) threshold to form an ECA-H<sub>2</sub>O nest, which is optimal in size and concentrations for initiation and polymerization to form polymer nanofibers. The diameter of the fibers above these critical threshold level remains unchanged (~50 nm) even as the axial rate of polymerization increases. Hence it is the subtle interplay of these surface thermodynamic and kinetics factors as caused by the interaction of water and adsorbed ECA which leads to templateless nanofiber synthesis.

## 5. Conclusions

In this report, we have demonstrated critical factors that underlie the template-less growth of PECA nanofibers on surface-modified glass surfaces. The premise established for the mechanism by which polymer nanofiber growth initiated on these surfaces entails the surface to be conducive for ECA monomer wettability. Once adsorbed on the surface, the ECA monomer is joined by water to form an optimal nest that

(21) Leonard, F.; Kulkarni, R. K.; Brandes, G.; Nelson, J.; Cameron, J. J. *J. Appl. Polym. Sci.* **1966**, *10*, 259–272.

(22) Plueddemann, E. P. *Silane Coupling Agents*, 2nd ed.; Plenum Press: New York, 1991.

(23) Kobayashi, H. *Makromol. Chem.* **1993**, *194*, 259–267.

forms the locus of polymer formation. For low concentrations of the water initiator (i.e., at low to moderate RH) only polymer buds were deposited, whereas in the presence of sufficient initiator concentration (moderate to high RH), polymer nanofibers were observed to form. When the substrate surface was thermodynamically unfavorable for ECA wetting (with low  $\gamma_c$ ), the rate of initiation of polymerization was relatively slower and the number density for polymer stubs was also low. The diameter and length of the polymer nanofibers, however, does increase above a certain humidity owing to a consistent thermodynamic interaction between ECA and water, in addition to increase in the overall rate of polymerization. The interplay of ECA and water must occur properly on any surface for initiation to take place. On the basis of the findings in this study, it is reasonable to envision new ways to control the extent of nanofiber formation by controlling the application of silanes

or carbonaceous deposit under humid conditions on glass or silicon. Additionally, ECA polymerization can continue as long as there is monomer present for continued fiber growth, thus facilitating bulk synthesis of these nanofibers. The control of placement during fabrication and the opportunity for bulk synthesis of nanofibers will prove to be important aspects of this chemistry if this technique is to be extended from the laboratory to application.

**Acknowledgment.** The authors acknowledge National Science Foundation NIRT Contract No. DM102-10229 for funding this research.

**Supporting Information Available:** Structures of silane molecules that were applied on Superclean\* glass slides and illustration of the enclosed chamber used for cyanoacrylate fuming (PDF). This material is available free of charge via the Internet at <http://pubs.acs.org>.

CM8022133